Visualizing shear bands in 3-D using axisymmetric sample: An experimental study

N.B. When citing this work, cite the original published paper.

(article starts on next page)

King Saud University

Journal of King Saud University – Engineering Sciences

www.ksu.edu.sa
www.sciencedirect.com

ORIGINAL ARTICLE

Visualizing shear bands in 3-D using axisymmetric sample: An experimental study

CrossMark

W. Khraisat [a],*, N.A. Rawashdeh [b], L. Nyborg [c]

[a] *Industrial Engineering Department, The University of Jordan, 11942 Amman, Jordan*
[b] *Mechatronics Engineering Department, German Jordanian University, 11180 Amman, Jordan*
[c] *Department of Materials and Manufacturing Technology, Chalmers University, SE-412 96 Gothenburg, Sweden*

Abstract In this study a qualitative description of the occurrence of shear bands produced by a sudden impact on an axisymmetric specimen made of medium carbon steel 0.45% C is given. A simple experiment was developed aimed at producing a pinch shear stress in the front side of the test sample in order to visualize shear bands in 3-D. Curve fitting using MATLAB was employed based on the points taken from the images of the front section of the test sample. The predictions of the curve fitting suggests a hyperbolic section leading to the conclusion that within the sample there is a double cone region of material where the shear band region is located on its outer surface. The formation of the shear band is explained by the fact that the interaction of the stress wave front with the free surface of the test sample produces reflection waves that attenuate the incoming stress wave inwards leading to a stress gradient in the plane of the front side of the specimen that causes shear localization. Also, the progressively increasing cross sectional area of the test sample causes the expansion of the wave front, which also results in a stress gradient in the normal direction of the front side of the specimen. So the formation of shear bands depends not only on the impact momentum and strain rates but also on the sample's geometry.

© 2015 The Authors. Production and hosting by Elsevier B.V. on behalf of King Saud University. This is an open access article under the CC BY-NC-ND license (http://creativecommons.org/licenses/by-nc-nd/4.0/).

1. Introduction

During severe deformation of ductile materials involving a large strain the mechanical properties of the material depend on the total strain and on the history of the strain path. A major characteristic is the appearance of flow lines. These lines can be thought of as lines that contain recognizable features like favourable grain orientation. During the forming methods the deformation history is composed of successive strain paths that vary in their orientation (Mathur and Dawson, 1989; Beyerlein and Tóth, 2009).

* Corresponding author. Tel.: +962 6 535 5000.
E-mail addresses: w.khraisat@ju.edu.jo (W. Khraisat), nathir.rawashdeh@gju.edu.jo (N.A. Rawashdeh), lars.nyborg@chalmers.se (L. Nyborg).

ELSEVIER | **Production and hosting by Elsevier**

In drop forging shear bands develop due to localization of deformation into narrow zones corresponding to the location of the maximum shear stresses (Wright, 2002; Zhu and Batra, 1990). These zones have a width of the order of several microns to several hundreds of microns (Voort, 1984).

In the experimental literature there are mainly three models on the onset criterion for shear bands. The first model is the thermal softening model which is based on the hypothesis that the onset of shear bands is attributed to local thermal softening (Zener and Hollomon, 1944; Dodd and Bai, 1992; Zhou et al., 2006; Zhang and Clifton, 2003). As a consequence of thermal softening, which is caused by a local rise in temperature, a region of the material will no longer harden, ultimately leading to strain localization.

The second model is the dynamic recrystallization model (DRX) which is based on the hypothesis that the dynamic stored energy initiates a dynamic recrystallization process of the deformed grains. The dynamic recrystallization will reduce the grain size to nano-scale causing local softening (Rittel et al., 2006; Medyanik et al., 2007).

The third model for explaining the occurrence of shear bands is the dislocation pile up model. Obstacles blocking the movement of dislocations lead to the accumulation of large strains in local regions (Armstrong and Zerilli, 1994; Clifton et al., 1984).

The main common points between these models are: (1) during dynamic loading, excessive strain is localized into the well known X-shaped region. This means that the shear band is found along the two sides of the cross section passing through the axis of loading. (2) The shear zone is a long and narrow zone of relative displacement contained between two parallel boundaries. The excessive strain is due to relative displacement across the shear band zone. However, there is no clear explanation on what causes this relative displacement and why does it occur across the X-shaped bands.

To obtain a complete picture of the shear bands developed in forged materials a 3-D visualization is needed. This is possible if the X-shaped region is brought out normal to the cross section passing through the axis of loading.

Stress waves induced in solid materials are a result from a sudden increase of pressure at intermediate strain rates from $1\,\mathrm{s}^{-1}$ to $10^2\,\mathrm{s}^{-1}$ (Cheng and Nasser, 2000; Jayaharia et al., 2014). The primary approach to testing in this strain rate range uses drop weight. In drop forging the drop weight occupies the entire upper surface of the test sample thus the shape of the wave front is planar and it is called a plane stress wave.

Assuming that homogeneous strain exists and a circle is inscribed in this region after deformation the circle will transform to an ellipse. Its longest and shortest radii define the principal strain axes. Material lines parallel to the principal axes undergo no shear strain. The principal strains are in line with the stretch along the principal axes. All grains are elongated along the flow lines, while they are compressed transverse to the flow lines. By constructing a circle in the undeformed region the amount of linear and angular strain involved in the deformation of the material can be related to the geometry of the resulting imaginary ellipse contained within the deformed material. By mathematical comparison with the original circle the radius of this ellipse is proportional to strain in any direction. Material lines parallel to the principal axes undergo no shear strain. Variation in strain path orientation during plastic deformation means that the principal axes of strain rotate. Thus, they do not remain in coincidence with the principal stress directions. These strain paths are called non-coaxial strain paths (Hsu, 1966).

The aim of this study is to develop an understanding of the formation of shear bands using axisymmetric samples to pinch out the X-shaped region as a means of visualizing shear bands in 3-D.

2. Experiments and results

The shape of the sample has been designed in order to pinch out the X-shaped structure. In order to do this a stress difference is needed between the area enclosed by the X-shaped structure and the area outside the X-shaped structure. To obtain this stress difference the shape of the test sample as shown in Fig. 1 has the shape of two truncated cones with a lower and upper radii of 52 mm and 30 mm respectively and a height of 35 mm. The L/D ratio of the sample is higher than 0.5 recommended by Davies and Hunter (1963). This is to lower friction effects between the specimen and the drop weight.

The stress wave attenuates as it propagates in a progressively larger volume. This increase in volume is made possible by the unsymmetrical geometry of the testing sample.

The shape of the test sample has been machined out from a cylindrical test specimen made of Swedish steel SS2244 (0.45% C, 1.02% Cr, 0.16% Mo). The two truncated cones sample was then cut into two halves along its longitudinal axis (y-axis). No attempts were made to remove scratches from the cutting step. These scratches will be used later to decide whether or not a

(a) Test sample as machined
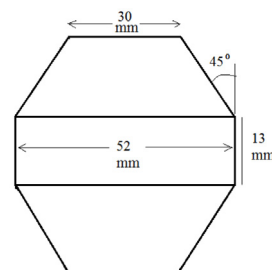
(b) Schematic of the test sample used

Figure 1   (a) Test sample as machined; (b) Schematic of the test sample used.

change in orientation occurs after drop forging in the area surrounding the pinched area.
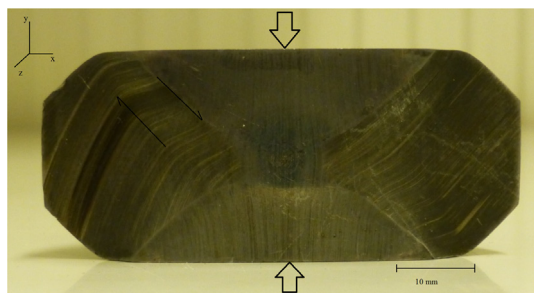
The drop hammer used in these experiments has a weight of 50 kg and it is raised to a height of 5 m. After the first deformation pass the front side of the sample developed a conical geometry as seen in Fig. 2. The pinched area was then polished and etched with 3% nital solution to reveal flow lines. The experiment was repeated several times and for each time the front side was pinched out even more and the flow lines did not change their orientation. The flow lines in the pinched area remained parallel to the compression stress axis (y-axis). However as forging proceeds a rectangular geometry was observed in the middle of the pinched area of the sample and within this geometry the flow lines bulge out radially.

A front view image of the forged specimen cross-section was used to numerically fit two branches of a hyperbola that are symmetrical about the vertical y-axis using MATLAB.
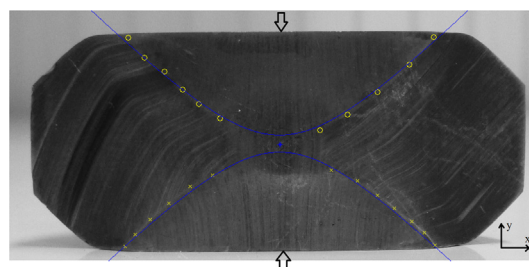
3. Discussion

By examining Fig. 2 it is obvious that part of the front side of the sample is pinched out. This is due to normal stress difference in the frontal direction of the sample (z-axis) where the magnitude of the normal stress in the pinched area differs from the normal stress in the unpinched surrounding area. The result of this stress difference between the pinched area and the surrounding area results in a simple shear stress operating on both borders of the shear band region.

By viewing the front side of the pinched area it can be considered as a conic section. Then, knowing that there are four kinds of conic sections, namely the parabola, the ellipse, the hyperbola and the circle; we can use the set of equations of conic section in order to determine the geometry of the resulting frontal surface (Dale, 2005). Essentially, the conics are obtained when a double cone is intersected by a plane. The cone has a circular horizontal cross section and a hyperbolic vertical cross section, which is evident from the pinched geometry of the test sample (see Figs. 2 and 3). Knowing that the hyperbola is centred at (0,0) the vertices are some fixed distance a from the centre. The foci of a hyperbola are inside each branch, and each focus is located at some fixed distance c from the centre and $a < c$ for any hyperbola. The standard equation of the hyperbola centred at the xy origin if the y-axis (the height of the sample) is the major axis is:

Figure 3 Fit of a hyperbola over the forged sample. The arrows represent compression direction.

$$\frac{y^2}{a^2} - \frac{x^2}{b^2} = 1 \qquad (1)$$

The foci are located at the y-axis and the asymptotes are the lines described by the equations:

$$y = \frac{a}{b}x \quad , \quad y = -\frac{a}{b}x \qquad (2)$$
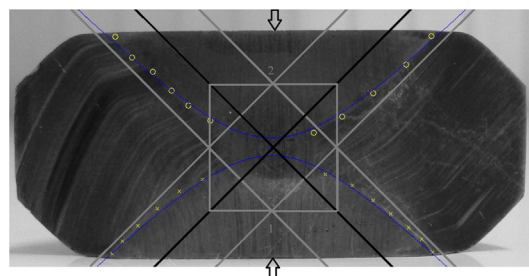
When the intersecting plane is parallel to the cone axis a rectangular hyperbola is obtained (Jolhe, 2008) and the asymptotes are perpendicular to one another. Experimentally, the angle between the X shaped shear band is known to be 90° (Zhu and Batra, 1990; Staudhammer et al., 2000). This means that the asymptotes which are in the same direction as the direction of the shear bands are also perpendicular. This corresponds to taking $a = b$ and plugging $a = b$ into Eq. (1) results in:

$$\frac{y^2}{a^2} - \frac{x^2}{a^2} = 1 \qquad (3)$$

and the asymptotes Eqs. will become:

$$y = x \quad , \quad y = -x \qquad (4)$$

In this study an attempt is made to get the best fit of points taken on the pinched geometry by using MATLAB. The result of this fit is shown in Fig. 3. It should be mentioned here that the resulting geometry is a result of a number of successive deformation passes. The experiment was repeated 8 times and after every deformation pass the rectangular part expands into the two branches of the hyperbola, which is evident from the bulged out flow lines seen in Fig. 2. The whole experiment was repeated 3 times using new samples and every time the front side of the sample is pinched out as seen in Fig. 2.

Figure 2 The pinched out geometry in the front side of the test sample. The arrows in the y direction represent compression direction. The two dark arrows indicate the shear stress at the boundary of the shear band.

Figure 4 The two branches of the hyperbola of the deformed sample with the grey asymptotes of the two branches having two different centre points 1 and 2 and the dark asymptotes having a common centre point (0,0).

In Fig. 4, the asymptotes for the two branches are drawn with grey colour. The centre points of the two branches are assigned with number 1 with coordinates (x_1,y_1) and number 2 with coordinates (x_2,y_2); which concludes that the two branches of the deformed sample have moved towards each other. The black asymptotes in Fig. 4, having a common centre point (0,0) belong to the hyperbola when no plastic deformation occurs. After every deformation pass the centre points of the two branches move away from the (0,0) point with a distance equivalent to the 'a' value of the branches.

Fig. 3 shows the hyperbolic fit with indicated coordinate system and sample face centre point (0,0). The centre points of the grey asymptotes and the cross points of the asymptotes define the dimensions of a square. The obtained square encloses the bulged-out flow lines.

The X-shaped pattern is a part of a geometry. The surface where the maximum shear stress occurs is thus on a cone surface. The cone is a developable surface meaning that its surface has the same tangent plane along a generator and since the normal to the surface is perpendicular to the tangent plane any normal to the surface along the generator is parallel to another normal to the surface (Aumann, 1991). This means that the shear bands orient themselves to maintain a fixed angle to the deformation axis. This finding in the present study seems to be consistent with one of the shear bands key characteristics (Cizek and Bai, 2004; Wagner et al., 1995). The shear band is inclined at 45° to the compression axis (y-axis) also by carefully examining Fig. 2 the shear band is shown to be inclined at 45° to the normal of the front surface of the test sample (z-axis). This means that whenever there is a stress gradient in a specific direction the shear band will be inclined to that direction at 45°.

This requires a continuous rotation of the interior of the shear band (Wagner et al., 1995).

By examining the scratch lines within the shear band it is evident that there is an offset (slip) across the shear band. The scratches on opposite sides of the shear band were originally continuous. Due to the relative displacement between the material on both sides of the shear band, deformation is concentrated in the shear band. Rotation of the scratch lines within the shear band region indicates that a simple shear mod is active. Simple shear hence results in a non-coaxial strain and then the scratch lines within the shear band will continuously rotate away from the border lines towards the central line of the shear band. As a consequence the angle composed of the scratch lines with the central line of the shear band will be less than the angle the scratch lines will make with the borders of the shear band. This implies that an imaginary ellipse within the shear band will rotate to a position where its major axis is parallel to the borders of the shear band. The material lines within the shear band will orient themselves towards parallelism where the strain is highest. Across the shear band region, a gradient of shear strain is developed which increases towards the borders of the shear band region. The grains will be oriented depending on their positions along the strain gradient.

The flow lines (material lines) within the pinched area remain longitudinal throughout the tests suggesting that the strain path is coaxial. The material structure oriented in the compression direction will change length but it will not change orientation (Burhanettin, 2006). The major and minor axes of an imaginary ellipse will not rotate, but all other lines will rotate. Thus, the mode of shearing is pure shear.

The impact between the drop weight and the flat surface of the sample generates a plane stress wave that propagates along the y-axis. At the samples boundary the stress wave front will not cross this boundary and instead be totally reflected back within the material due to the large impedance mismatch (Aumann, 1991). The free surface reflections generate rarefaction waves that superimpose on the original stress wave form.

It is reasonable to propose that due to the fact that the already formed shear band from the previous deformation pass is at an angle with the loading axis (y-axis), the shear band will experience an oblique impact from the new incident stress wave. When the incident wave encounters the boundary of the shear band, part of the wave is reflected from the boundary. This is a result of the difference in compressibility between the material within the shear band and that of the surrounding material. The reflections interfere with the original wave, producing patterns of destructive interference and a new shear band is formed. The newly formed shear band will be along the boundary of the previously formed shear band. The shear band region thickness increases due to multi passes of deformation. As the thickness of the shear band region increases so also will the oblique impact on the expense of the normal impact.

4. Conclusions

In this work we propose a new criterion leading to shear localization. It is believed that the impact loading generates a plane stress wave that propagates along the y-axis and at the sample boundary the wave front will be totally reflected back internally due to the large impedance mismatch. The reflected wave interferes with the original shock producing patterns of destructive interference. The stress wave propagating through the sample can be considered as being divided into two segments across the shear band. The first segment is within the conical section and the second segment outside the conical section. The two segments will have different amplitudes however the amplitude within each segment of the stress wave will be constant everywhere on the plane perpendicular to its direction of travel.

References

Armstrong, R.W., Zerilli, F.J., 1994. Dislocation mechanics aspects of plastic instability and shear banding. Mech. Mater. 17, 319–327.

Aumann, G., 1991. Interpolation with developable bezier patches. Comp. Aid. Geo. Des. 8, 409–420.

Beyerlein, I.J., Tóth, L.S., 2009. Texture evolution in equal-channel angular extrusion. Prog. Mater Sci. 54, 427–510.

Burhanettin, A., 2006. Severe Plastic Deformation: Toward Bulk Production of Nanostructured Materials, first ed. Nova Science, Michigan.

Cheng, Jingyi., Nasser, Sia., 2000. A model for experimentally-observed high strain-rate dynamic strain aging in titanium. Acta Mater. 48, 3131–3144.

Cizek, P., Bai, F., Rainforth, W., Beynon, J., 2004. Fine structure of shear bands formed during hot deformation of two austenitic steels. Mater. Trans. 45, 2157–2164.

Clifton, R.J., Duffy, J., Hartley, K.A., Shawki, T.G., 1984. On critical conditions for shear band formation at high strain rates. Scr. Metall. 18, 443–448.

Dale, P., 2005. Introduction to Mathematical Techniques used in GIS. CRC Press, Florida.

Davies, E., Hunter, C., 1963. The dynamic compression testing of solids by the method of the split Hopkinson pressure bar. J. Mech. Phys. Sol. 11, 155–179.

Dodd, B., Bai, Y.L., 1992. Adiabatic Shear Localization: Occurrence, Theories, and Applications. Pergamon Press, UK, Oxford.

Hsu, T.C., 1966. The characteristics of coaxial and non-coaxial strain paths. J. Strain Anal. Eng. Des. 1, 216–222.

Jayaharia, L., Sasidhara, P.V., Prudvi Reddya, P., BaluNaikb, B., Guptac, A.K., Singha, Swadesh Kumar, 2014. Formability studies of ASS 304 and evaluation of friction for Al in deep drawing setup at elevated temperatures using LS-DYNA. J. King Saud Univ. 26, 21–31.

Jolhe, D., 2008. Engineering Graphics. Tata McGraw-Hill, New Delhi.

Mathur, K., Dawson, P., 1989. On modeling the development of crystallographic texture in forming processes. Int. J. Plasticity 5, 67–94.

Medyanik, N.S., Liu, W.K., Li, Shaofan., 2007. On criteria for dynamic adiabatic shear band propagation. J. Mech. Phys. Sol. 55, 1439–146.

Rittel, D., Wang, Z.G., Merzer, M., 2006. Adiabatic shear failure and dynamic stored energy of cold work. Phys. Rev. Lett. 96, 075502.

Staudhammer, K., Murr, L., Meyer, M., 2000. Fundamental Issues and Applications of Shock Wave and High Strain Rate Phenomena. Elsevier Science Ltd, UK.

Voort, G., 1984. Metallography: Principles and Practice. ASM International, McGraw-Hill Book Co., New York.

Wagner, P., Engler, O., Lucke, K., 1995. Formation of Cu-type shear bands and their influence on deformation and texture of rolling fcc {112} <111> single crystals. Acta Metall. Mater. 43, 3799–3812.

Wright, T.W., 2002. Physics and Mathematics of Adiabatic Shear Bands. Cambridge University Press, UK.

Zener, C., Hollomon, J., 1944. Effect of strain rate on plastic flow of steel. J. Appl. Phys. 15, 22–32.

Zhang, Z., Clifton, R.J., 2003. Shear band propagation from a crack tip. J. Mech. Phys. Sol. 51, 1903–1922.

Zhou, F., Wright, T.W., Ramesh, K.T., 2006. A numerical methodology for investigating the formation of adiabatic shear bands. J. Mech. Phys. Solids 54, 904–926.

Zhu, Z.G., Batra, R.C., 1990. Dynamic shear band development in plane strain compression of a viscoplastic body containing a rigid inclusion. Acta Mech. 84, 89–107.